

The decay time scale for highly excited nuclei as seen from asymmetrical emission of particles

M. Jandel^{a,b}, A.S. Botvina^{a,c}, S. J. Yennello^a, G. A. Souliotis^a,
D. V. Shetty^a, E. Bell^a, A. Keksis^a

^a*Cyclotron Institute, Texas A&M University, College Station, TX 77843, USA*

^b*Institute of Physics, Slovak Academy of Sciences, Dubravska 9, 84228 Bratislava,
Slovakia*

^c*Institute for Nuclear Research, Russian Academy of Science, 117312 Moscow,
Russia*

Abstract

A novel method was developed for the extraction of short emission times of light particles from the projectile-like fragments in peripheral deep-inelastic collisions in the Fermi energy domain. We have taken an advantage of the fact that in the external Coulomb field particles are evaporated asymmetrically. It was possible to determine the emission times in the interval 50-500 fm/c using the backward emission anisotropy of α -particles relative to the largest residue, in the reaction $^{28}\text{Si} + ^{112}\text{Sn}$ at 50 MeV/nucleon. The extracted times are consistent with predictions based on the evaporation decay widths calculated with the statistical evaporation model generalized for the case of the Coulomb interaction with the target.

Key words: Time Scale, Projectile Fragmentation, Nuclear Evaporation, Coulomb Excitation

PACS: 25.70.Mn, 25.70.De, 24.60.-k

1 Introduction

Strong external fields may substantially change the nature of physical processes as compared to ones which occur in an isolated environment. Studies of electromagnetic processes in relativistic heavy-ion collisions (see e.g. [1,2])

¹ E-mail address: jandel@comp.tamu.edu

and references therein), demonstrate the possibility of a large energy transfer to nuclei. It is natural that similar electromagnetic processes may occur for heavy ion collisions near the Fermi energy. In the case of deep-inelastic peripheral nucleus-nucleus collisions, the electromagnetic interaction is small compared to the nuclear one, however, it may provide an important contribution to fragment production leading to new effects. For example, as was pointed out in refs. [3,4], the fast multifragmentation of projectile-like and target-like sources is influenced by the Coulomb interaction between them, and this interaction leads to asymmetrical emission of intermediate mass fragments from the sources.

The interplay between electromagnetic and nuclear forces should be also manifested in other phenomena. The evaporation of isolated nuclei is well described by present theories [5,6]. However, in the case of collisions of nuclei, one may expect that the de-excitation of the projectile takes place in the vicinity of the target. In the peripheral deep-inelastic collisions, when the projectile-like nucleus acquires excitation energies $E^* \sim 3-5$ MeV/nucleon, the fast evaporation takes place on a time scale of 10^{-22} s (50-500 fm/c). In this paper, we consider the effect of asymmetrical light particle evaporation, which may appear as a consequence of the Coulomb interaction between the highly excited nuclei that decay rather quickly in the vicinity of each other. We demonstrate that this effect can be used for determination of the decay time of these nuclei, as was previously discussed in ref. [7].

2 Experimental observation

We reanalyzed the data obtained in the peripheral reactions of ^{28}Si with ^{112}Sn at 50 MeV/nucleon [8]. The excited projectile-like source (PLS) was carefully reconstructed on event-by-event basis. We considered events containing the largest residue charge $Z(LR) \geq 7$ and light charged particles, having the total charge of the reconstructed projectile-like source $Z(PLS) = 13$ and 14. These products are in the kinematics region of the projectile, with the laboratory velocities around $v \approx 0.3c$. We concentrate on events having α -particles, since these particles are usually produced in the evaporation process.

The isotopic resolution in the experiment was achieved only for $Z \leq 5$ and no free neutrons were detected. The reconstruction of the projectile-like source excitation energy is therefore influenced by the uncertainty in the determination of the mass of projectile-like source. However, in this work, the mass assumption for $Z > 5$ fragments used in the experimental data was applied to the simulation. Additionally, neutrons are omitted when reconstructing the excitation energy so that the simulated and experimental values of the excitation energy match. In this manner, we defined the apparent excitation

energy

$$E_{app}^* = \sum_i (T_i^{PLS} + \Delta M_i) - \Delta M_{PLS}, \quad (1)$$

where T_i^{PLS} are the kinetic energies of the fragments in c.m.s. of the projectile-like source, ΔM_i are the mass excesses of fragments and ΔM_{PLS} is the mass excess of the projectile-like source. The angular distribution of α -particles was extracted from parallel and perpendicular velocities in the reference frame of the heaviest fragment, (which in our case was limited to $Z \geq 7$ to assure projectile-like events).

Fig. 1 shows the scatter plots and angular distributions of emitted α -particles relative to the largest fragment, for reconstructed projectile-like events with the charge $Z(PLS) = 14, 13$ in the reaction $^{28}\text{Si} + ^{112}\text{Sn}$ at 50 MeV per nucleon. The asymmetrical emission is clearly observed. We performed the additional selection of events inside the Coulomb circle (shown by lines in the scatter plots in Fig. 1a, c), in order to be more stringent and restrict our analysis exclusively to the projectile-like evaporation process and avoid contributions from other processes. The asymmetrical emission is still present as shown by dotted spectra in Fig. 1b, d.

Fig. 2 shows the distribution of the PLS apparent excitation energy for the events in the Coulomb circle and how the angular asymmetry of emitted α -particles changes with the excitation energy. The backward emission of α -particles prevails over the central and forward emission, for all four bins of E_{app}^* and more importantly, the asymmetrical emission is increased with the excitation energy.

In order to estimate the angular asymmetry of α -particles, we defined three regions of emission: backward = $\cos \theta \in \langle -0.81, -0.27 \rangle$, central = $\cos \theta \in \langle -0.27, 0.27 \rangle$ and forward = $\cos \theta \in \langle 0.27, 0.81 \rangle$. As a reference parameter in our analysis, we will use the ratio of backward to central emission

$$bc = \frac{N(\textit{backward})}{N(\textit{central})}. \quad (2)$$

The choice of the regions was influenced by the fact that the experimental efficiency of detecting both the heaviest residue and the α -particle in the same detector is small. This can be, in fact, seen from the angular distributions shown in the lower panel of Fig. 2, where we observe the drop of events in the region of $|\cos\theta| > 0.8$. Therefore, α -particles in the angle range $|\cos\theta| > 0.8$ were excluded from further analysis.

3 Theoretical interpretation

The sequential particle evaporation from hot nuclei is a quite reliable approach for the description of experimental data at excitation energies $E^* \lesssim 3\text{-}5$ MeV/nucleon. In peripheral nucleus–nucleus collisions the evaporation process may be very fast and proceed when the PLS and the TLS (target-like source) are not far away from each other. Therefore, the evaporation of particles from both excited sources happens in the common Coulomb field. To examine the main features of Coulomb proximity decay, we have constructed a model in which the PLS with mass number A and charge Z , characterized by a spin and excitation (E^*), moves away from TLS with velocity V . At a given separation distance the de-excitation of PLS via sequential binary decay of light particles (n , $Z \leq 2$) and heavy clusters (up to ^{18}O) is calculated using a Weisskopf approach [5]. In this model [9], the decay width for the emission of a particle j in the excited state i from a nucleus with (A, Z) is given by:

$$\Gamma_j^i = \int_0^{E_{CN}^* - B_j - \epsilon_j^{(i)}} \frac{\mu_j g_j^{(i)}}{\pi^2 \hbar^2} \sigma_j(E) \frac{\rho_f(E_{CN}^* - B_j - \epsilon_j^{(i)} - E)}{\rho_{CN}(E_{CN}^*)} E dE \quad (3)$$

Here $\epsilon_j^{(i)}$ ($i = 0, 1, \dots, n$) are the energies of the ground and all particle-stable excited states of the fragment j , $g_j^{(i)} = (2s_j^{(i)} + 1)$ is the spin degeneracy factor of the i -th excited state, μ_j and B_j are the corresponding reduced mass and separation energy, E_{CN}^* is the excitation energy of the initial compound nucleus (i.e. PLS), and E is the kinetic energy of an emitted particle. The level densities of the initial compound (A, Z) and the final (A_f, Z_f) residual nucleus, ρ_{CN} and ρ_f , are calculated using the Fermi-gas formula $\rho(E) \propto \exp(2\sqrt{aE})$ with the level density parameter $a \approx 0.15A\text{MeV}^{-1}$ corresponding to the nuclei with $A \approx 20 - 30$. In the present work, we have parametrized the inverse cross section as $\sigma_j(E) = \pi R_{fj}^2 (1 - U_c/E)$, where U_c is the Coulomb barrier for fragment emission and $R_{fj} = R_f + R_j$, $R_f = r_0 A_f^{1/3}$, $R_j = r_0 A_j^{1/3}$, with $r_0 = 1.5\text{fm}$.

We assume that the electromagnetic interaction between TLS and PLS influences each evaporation act. The transformation of the Coulomb energy into nuclear one (and vice versa) can be described within different approaches. Previously, in multifragmentation reactions, this problem was resolved by taking into account the whole coordinate phase space of the produced fragments [3]. The phase space analysis is model-independent and it can also be applied for our evaporation case. However, for better physics understanding of the phenomenon, it is useful to consider a particular model process. Therefore, we suggest that the TLS Coulomb field leads to a shift of the proton distribution with respect to the neutron one in PLS. This means that the PLS charge

center can be shifted from the PLS center-of-mass. A similar process of a dipole charge polarization is well known in electromagnetic interactions with nuclei as a Goldhaber-Teller and Steinwedel-Jensen giant resonances [10,11]. Since the evaporation rate is very fast at high excitation energies, the charge distribution of the evaporated particle and the residue should correspond to this 'dipole' shift of the PLS charge distribution. We consider different positions of the charge centers of the evaporated daughter's α and the residual by assuming them to be touching charged spheres, which are placed within a sphere of radius $R_j + R_f$ with the center located at the center-of-mass of the decaying (PLS) nucleus. These coordinate positions are simulated with the Monte-Carlo method. In this case the shifts of the PLS charge center (~ 1 fm) match rather well to the displacements of the neutron and proton distributions expected in giant resonances [10]. The corresponding shift of the neutron distribution of the residue may preserve the PLS center-of-mass conservation during the decay. This is consistent with the fact that the PLS residue remains excited and it can also be dipole-like deformed in the external Coulomb field. However, we note that the PLS center-of-mass conservation is not an obligatory requirement, contrary to the case of a two-body evaporation of an isolated nucleus, because of an energy transfer from the external Coulomb to the nuclear deformation of PLS during the decay. While the center-of-mass of the whole three-body system (TLS, the residue and the daughter fragments) must be conserved during the evaporation, as it is in our model. In this paper we are limited to a qualitative description of this new kind of emission, and we do not develop the model further (e.g., there should be a connection between the magnitude of the dipole polarization and the symmetry energy of nuclei at high excitation energies, which can be addressed in these processes). Also, the scope of this paper does not include other consequences of the dipole polarization, like a possible neutron enhancement of particles emitted toward TLS.

Within this approach the decay configuration is impacted by the change in the Coulomb energy of the three-body system:

$$U_c = \left(\frac{Z_f Z_j}{R_{fj}} + \frac{Z_{TLS} Z_j}{R_{TLS-j}} + \frac{Z_{TLS} Z_f}{R_{TLS-f}} - \frac{Z_{TLS} Z}{R_{TLS-CN}} \right) e^2, \quad (4)$$

where Z_{TLS} is the charge of TLS, R_{TLS-CN} is an initial distance from the TLS to the compound nucleus, and R_{TLS-j} (R_{TLS-f}) is a distance from the TLS to the charge center of the emitted particle j (the residue f), which takes also into account the TLS fluctuations guaranting the center-of-mass conservation of the three-body system, respectively. The probability of fragment emission can be found by averaging eq. (3) over all coordinates of the charge centers of fragments. Since the Coulomb energy is lower when fragment j is emitted in the direction of the TLS, the resulting fragment emission is anisotropic in the PLS frame. The angular momentum of the PLS was included using a standard

approach [4,12].

The width for evaporation of particle j is $\Gamma_j = \sum \Gamma_j^i$, and the full width is determined by summing up all emission channels: $\Gamma = \sum \Gamma_j$. By definition we take the mean time for an emission step as $\tau = \hbar/\Gamma$. The PLS is assumed to have a lifetime, t , with a distribution $\exp(-t/\tau)$. Until the decay occurs, the PLS, TLS, and all charged particles propagate along Coulomb trajectories. Successive binary emissions, conserving energy and momentum, are calculated until the excitation energy is below the particle emission threshold. In the case of this reaction, we do not take into account the Coulomb influence of the previously emitted particles on probabilities of subsequent emissions, because the large charge of the TLS dominates.

4 Discussion of the results

After separation of the PLS and the TLS, the emission rates for particles and their angular distributions depend on excitation energies and distances between them. Fig. 3 shows the calculated scatter plots and angular distributions of emitted α -particles for different excitation energies at a fixed distance (20 fm). The effect becomes more pronounced at lower energies since the Coulomb energy surplus becomes more essential. However, according to the calculations, at low excitation energy the decay time is large, so the distance can not be small. In this respect, we have a well defined problem: to find the right distances at which the decay occurs in order to describe the observed angular anisotropy. Since we know the relative PLS-TLS velocity, one can easily connect them with the decay time. The finite size of the TLS and the fluctuations of the coordinates of the emitted particle and the residue as a result of the evaporation were taken into account. However, the corresponding corrections are not essential at large distances and do not influence the obtained trends.

Fig. 4a shows the experimental angular anisotropy parameter bc , observed for different apparent excitation energy bins. Fig. 4b demonstrates how the calculated ratio bc changes with the distance at which the first emission (after separation of PLS and TLS) happens for four initial excitation energies of ^{29}Si ($E^* = 2.5, 3, 3.5$ and 4 MeV/nucleon). After recalculation of the apparent excitation energy according to (1) (the values of apparent excitation energies in calculation are shown in Fig. 4b), one can directly compare the asymmetric parameter values bc and extract the distances at which the first emission occurs for the corresponding apparent excitation energy. The time of the emission is then determined from the separation distances of PLS-TLS divided by their relative velocity. The time of the first emission is shown in Fig. 5 for Si and Al. For illustration, we show the evaporation times calculated according to the

widths found in the model for ^{29}Si and ^{27}Al . A rapid lifetime drop with the excitation is a general behavior of evaporation lifetimes (see also, e.g., [13]), and it reflects a gradual transition to simultaneous multifragment decay, which has been discussed in the literature [14]. One can see a qualitative agreement for the extracted and the calculated times. Improvements in model parameters and selection of an isotopic distribution of sources should result in even better agreement, however the primary goal of the present study is to demonstrate the possibility of this method.

We emphasize, that in our analysis we exclude α -particles with $v > |0.1c|$, in order to guaranty a selection of an evaporation-like process. The energy spectra of these particles can be explained by a normal evaporation emission (see also [7]). While one may speculate that the asymmetry is induced by the previous dynamical stage there are currently no dynamical models which are able to describe this process. The dynamical emission is usually associated with particle production at midrapidity velocities, which are excluded from our analysis. We expect that the time for a dynamical emission is rather short $\lesssim 50$ fm/c, while the present method is aimed at the decay times ≈ 50 -500 fm/c, where an equilibration is quite probable. Additionally, equilibrium is to be expected because of the relatively low energy released during emission of one particle (i.e. just slightly above the threshold energy for α emission), in comparison with a large energy transferred during the collision process. Therefore, it is a reasonable explanation that this phenomenon can occur as a joint effect of nuclear and electromagnetic forces during the fast decay of PLS in the proximity of TLS.

We note that the Coulomb proximity effect of evaporative alphas in the direction between the two larger fragments was already reported for fission events [15]. However, in this previous work it was not possible to explain fully the magnitude of this effect. In our new interpretation an enhancement of the 'midrapidity' evaporation is connected with a dipole-like charge deformation inside the nucleus, which can lead to the creation of a new minimum in the potential energy at the moment of evaporation in the presence of the third charged body. In this way, the external Coulomb energy is converted into internal energy of the source.

5 Conclusions

We have considered the evaporation-like decay of highly excited projectile nuclei produced in peripheral nucleus-nucleus collisions. The time for production of these nuclei can be estimated as ≤ 50 fm/c (the time of separation of the projectile and target nuclei). Afterwards, the nuclei undergo rapid de-excitation. We demonstrated that this decay has a large angular asymmetry, which is

not expected for the standard evaporation process. As was pointed out, the physical condition at which this evaporation happens is different from the evaporation from an isolated compound nucleus. Since the decay is very fast the target is still in the vicinity of the decaying projectile nucleus, and their Coulomb interaction influences the decay. This effect can explain the observed asymmetry, as was shown by comparison with our model. One can connect the observed asymmetry with the distance between the target and the projectile and consequently with the decay time. In this respect, the "proximity decay" may be considered as a "clock" sensitive to the times of 50-500 fm/c, during which this proximity exists. To our knowledge, these are the smallest decay times which can be identified in a sequential framework. At higher excitation energies, we expect a simultaneous multifragment decay into many small fragments.

6 Acknowledgements

The authors wish to thank the staff of the Texas A&M Cyclotron facility for the excellent beam quality. This work was supported in part by the Robert A. Welch Foundation through grant No. A-1266, and the Department of Energy through grant No. DE-FG03-93ER40773. We thank R. De Souza, L. Sobotka, R. Charity and S. Hudan for stimulating discussions.

References

- [1] C.A.Bertulani and G.Baur, *Phys. Rep.*, **163**, 299 (1988).
- [2] I.A. Pshenichnov et al., *Phys. Rev.* **C57**, 1920 (1998)
- [3] A.S.Botvina, M.Bruno, M.D'Agostino and D.H.E.Gross, *Phys. Rev.* **C59**, 3444 (1999).
- [4] A.S. Botvina and I.N. Mishustin, *Phys. Rev.* **C63**, 061601(R) (2001).
- [5] V. Weisskopf, *Phys. Rev.*, **52**, 295 (1937)
- [6] T. Ericson, *Adv. in Phys.*, **9**, 425 (1960).
- [7] S. Hudan et al., *nucl-ex/0308031*, (2003)
- [8] A. Laforest et al., *Phys. Rev.* **C59**, 2567 (1999).
- [9] A.S. Botvina et al., *Nucl. Phys.* **A475**, 663 (1987).
- [10] M. Goldhaber and E. Teller, *Phys. Rev.* **74**, 1046 (1948).
- [11] H. Steinwedel and H. Jensen, *Z. Naturforsch.* **5A**, 413 (1950).

- [12] R.J. Charity et al., Nucl. Phys. **A483**, 371 (1988).
- [13] R.J. Charity et al., Phys. Rev. **C61**, 054614 (2000).
- [14] L. Beaulieu et al., Phys. Rev. Lett. **84**, 5971 (2000).
- [15] A. Brucker et al., Phys. Lett. B, **186**, 20 (1987).

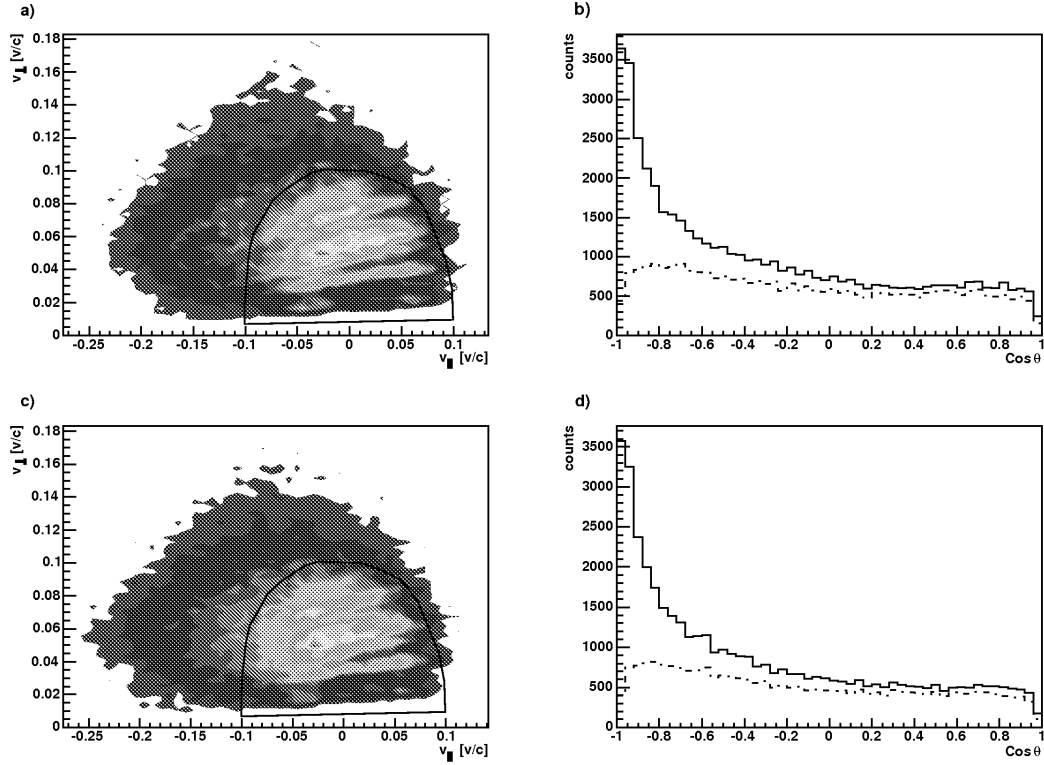


Fig. 1. Velocity scatter plots of ^4He particles emitted from the PLS (a,c) and angular distributions of α -particles (b,d) from the reaction $^{28}\text{Si} + ^{112}\text{Sn}$ at 50 MeV/nucleon. Angular distributions shown by dotted lines correspond to α -particles emitted within the Coulomb circle (shown by continuous line in the scatter plots). Solid line represents all α -particles from events that met the sum Z(PLS) criterion. The results for Z(PLS)=14 and Z(PLS)=13 are shown on the top and bottom, respectively.

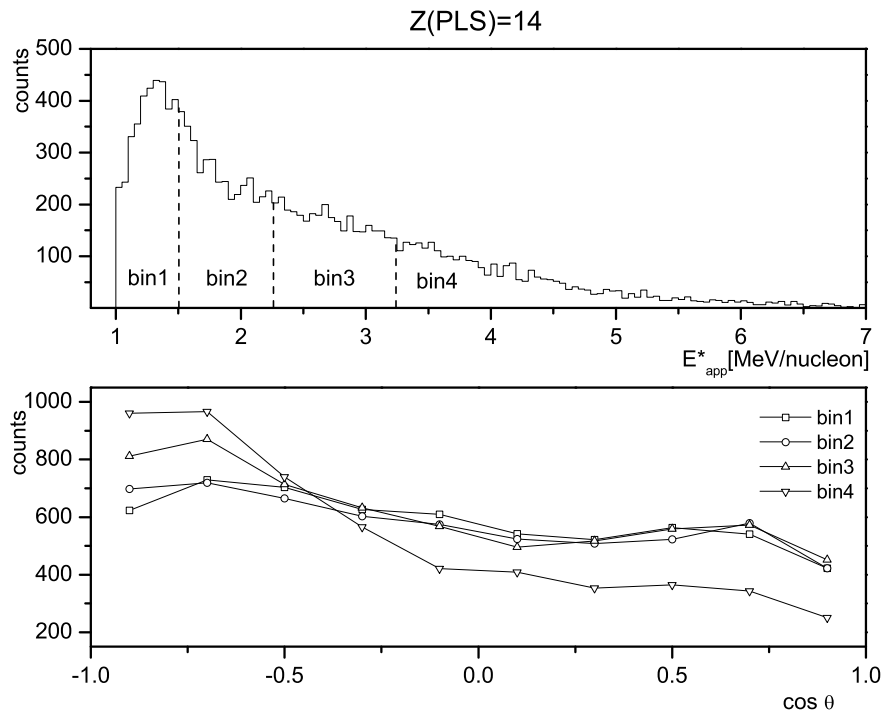


Fig. 2. The distribution of apparent excitation energy E_{app}^* of reconstructed projectile-like sources with the sum charge $Z(PLS)=14$ (upper) and angular distributions of α -particles in the c.m.s. of projectile-like fragment (lower) for selected E_{app}^* bins.

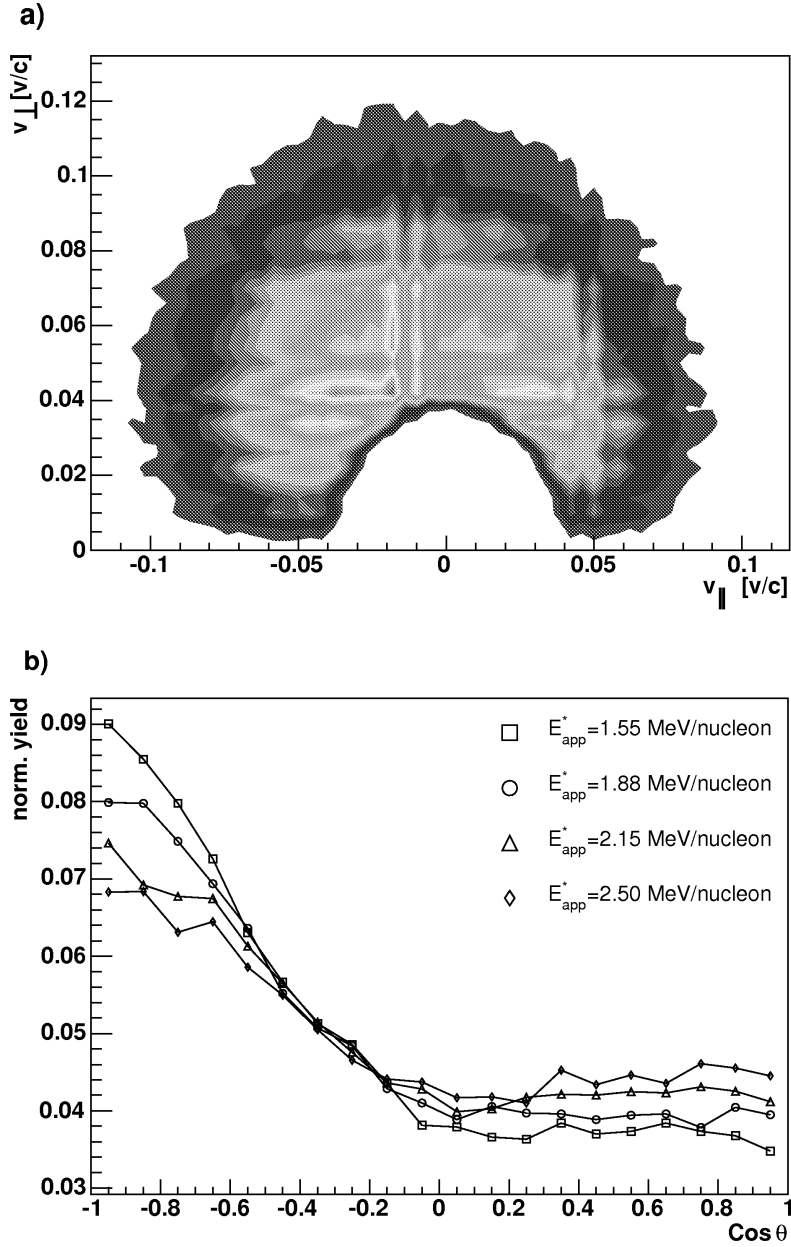


Fig. 3. Velocity scatter plot of α -particles (a) and angular distribution of α -particles (b) obtained from calculations of proximity decay of ^{29}Si at 20 fm and apparent excitation energies $E_{app}^* = 1.55, 1.88, 2.15$ and 2.50 MeV.

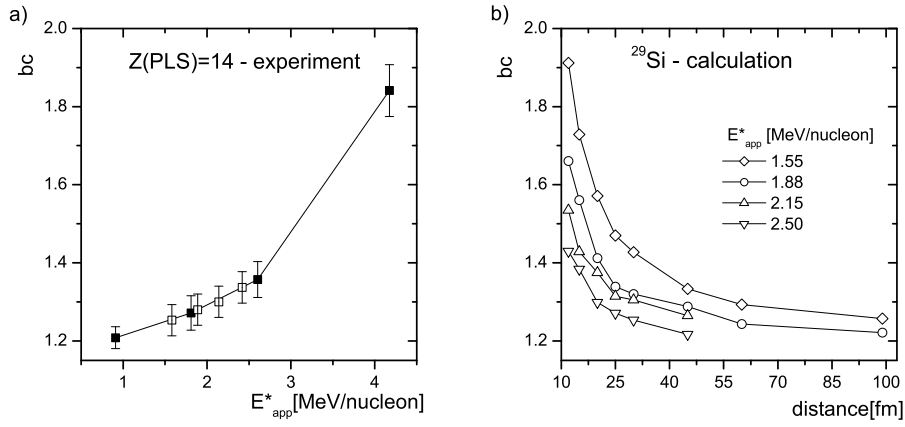


Fig. 4. Anisotropy parameter bc as a function of the apparent excitation energy E_{app}^* obtained from experimental data - (a), and calculated values of anisotropy parameter bc as a function of the distance for different E_{app}^* - (b). Empty squares in (a) show estimated values of bc parameter for E_{app}^* involved in the calculation shown in (b).

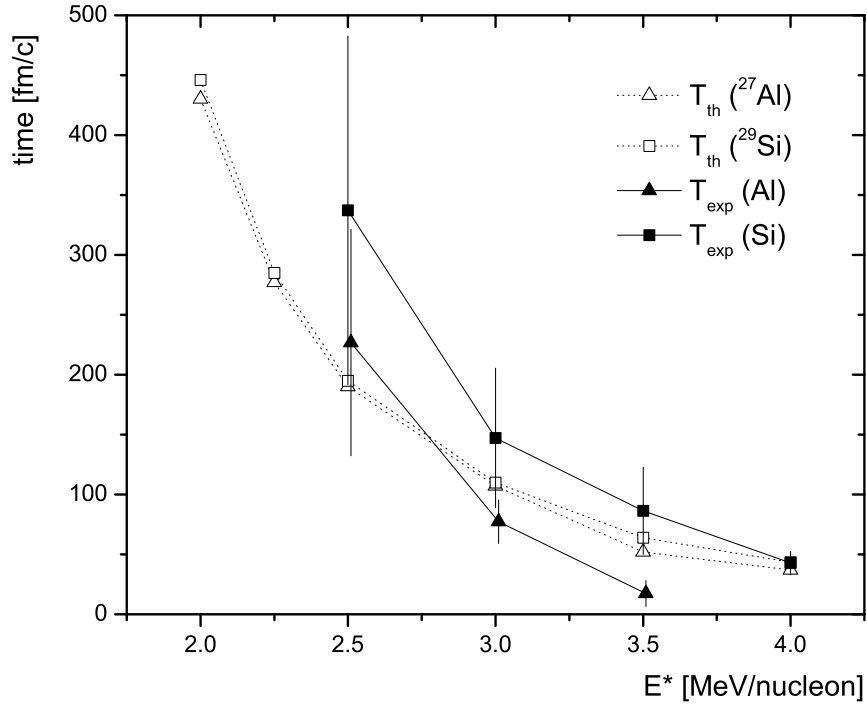


Fig. 5. Time of the first emission T_{exp} obtained by comparison of angular anisotropy parameter bc observed in experiment (full symbols). Time of the emission T_{th} calculated from total decay width is shown for comparison (empty symbols). Square and triangle symbols correspond to results for $Z(\text{PLS})=13$ (Si) and $Z(\text{PLS})=13$ (Al), respectively.